BARCHAN MORPHOMETRY:

EXAMPLES FROM EARTH AND MARS

by

ROBERT JACK BUTLER

DOUGLAS J. SHERMAN, COMMITTEE CHAIR
DAVID J. KEELLINGS
JEAN T. ELLIS

A THESIS

Submitted in partial fulfillment of requirements
for the degree of Master of Science
in the Department of Geography
in the Graduate School of
The University of Alabama

TUSCALOOSA, ALABAMA

2019

ABSTRACT

Barchans are a common sand dune type found on both terrestrial and Martian surfaces. The morphometry of individual barchans and barchan groups has been measured extensively in past studies. Within each dune field, similar sized barchans are observed to be abundant, but previous morphometric studies typically do not compare their results with those from many other dune fields. This study includes diverse dune fields on both Earth and Mars concentrating mostly on the dimensionless geometric variabilities of their barchan populations. The geometries show a degree of similarity between barchan populations despite the different environmental characteristics from one dune field to another. This project made use of NASA's public photos, Mars Reconnaissance Orbiter CTX Imagery, Google Earth, and Digital Globe's free, high-resolution imagery. The key dimensions of more than 1500 barchans, representing dunes from 14 terrestrial and 5 Martian dune fields, were measured using the Google Earth ruler tool and Photoshop CC software. Determining the variation of barchan geometry provides evidence of similar barchan characteristics on a large scale and creates a foundation for future research. Documenting these barchan geometries provides a better understanding of the geomorphic time-space sequences, evolutions, geospatial distributions of barchan populations, and may provide a robust basis for the classification of barchan morphologies according to dimensionless geometry.

DEDICATION

Dedicated to my wife Jenna. Without her endless support, patience, and love, this would not have been possible. Thank you for always being by my side and never giving up on me.

ACKNOWLEDGMENTS

First, I would like to thank Dr. Douglas Sherman, the chairman of this thesis, for being patient and having faith in me throughout these past few years. Dr. Sherman has been encouraging and supportive in all aspects of my academic career, and I am honored to have had the chance to work under him. Additionally, I would like to thank my committee members, Dr. David Keellings and Dr. Jean Ellis, for their help, support, and flexibility throughout the duration of this project. I would also thank my parents for all the love and support they have given me throughout my years of schooling, and for always encouraging me to reach further than I thought I could. Lastly, I thank my friends and all the other faculty members at the University of Alabama Department of Geography for all the help they provided when it was needed.

CONTENTS

LIST OF TABLES

LIST OF FIGURES

INTRODUCTION

Formation and Features

The motivation for this research was inspired by the appearance of similarly sized barchans within most dune fields and by the limited presence of small barchan populations. We compared multiple diverse dune fields from Earth and Mars using the dimensionless geometric variability of their barchan populations. This allowed us to test the degree of similarity between the fields, despite different environmental characteristics, while providing a better comprehension of the space- time relationship.

Sand dunes are abundant across many planetary surfaces. Barchans, a common dune found in aeolian environments, have been observed on both Earth and Mars. Most dune types usually form under multidirectional winds, while barchans tend to reflect a nearly unidirectional wind flow (Parteli et al., 2009). Initially, winds lift the sand grains and eventually deposit them downwind forming a sand pile. Given enough time and the right conditions, a crescentic shaped dune called a barchan will emerge. Most barchan fields on Earth are composed of well sorted feldspars and quartz, with a select few composed of carbonates and gypsum (Bourke et al., 2010). Barchans usually form in locations that are flat, deprived of sand and vegetation, and not obstructed by topographic obstacles (Breed et al., 1979). A typical barchan profile can be viewed in the appendix under Figure 1.

The windward side of a barchan is known as the stoss slope, while the downwind side is known as the lee side. The stoss slope extends from the most upwind base of the windward side to the brink line or crest. Stoss slopes tend to usually maintain an angle between 2 and 20 degrees (Dong et al., 2007; Lancaster, 1995). The highest point of a barchan is the crest.

The crest is located on the downwind side of the stoss slope near the brink line. If the crest is not visible on a barchan, then the pinnacle of the brink line and the crest are the same. Barchans of similar height may be present in the same dune field with and without crests (Bourke and Goudie, 2009; Andreotti et al., 2002; Hesp and Hastings, 1998). The brink line divides the windward side from the lee side of a barchan and is where an eddy develops and sand grains come to rest near the top of the slip face (Hersen, 2004). When the wind applies enough shear stress over a dunes surface the sand grains will be dislodged and transported through a process called saltation and reptation to the lee side of the dune. The slip face and horns make up the lee side of a barchan. The upper slip face of a barchan will accumulate sand until it reaches the repose angle, or the maximum angle at which a sedimentary slope is stable. The angle of repose for a barchan can usually be observed between 30 and 35 degrees with an average around 32 degrees (Pelletier et al., 2015; Sutton et al., 2013a; Sutton et al., 2013b). The slip face has a critical angle near the brink and a lower angle near its base. These angles represent the degree in which a slope can increase before avalanching, and the degree in which the sand settles after the avalanche has already occurred (Pelletier et al., 2015). The horns of a barchan form along the dune's sides and point in the downwind direction. Sand from the windward side help the horns replenish and potentially grow larger if the influx is greater than the outflux. Alternatively, if the outflux is greater, then the dune will slowly lose mass over time and the horns will reduce in size. A barchans sand loss occurs at the tip of the horns. After grains traverse across the windward side of the dune toward the end of the horn, the sand then leaks from the horn tip in the downwind direction. The sediment loss at the tip of the horns occurs at varying rates and usually helps provide an influx of sand to the next dune downwind.

Barchan Size

Barchans observed in nature are found in many different sizes. These crescent-shaped dunes are usually wider than they are long, and display an asymmetric figure (Tsoar and Parteli, 2016). The asymmetric figure may be due to an asymmetric sediment supply (Zhang et al., 2018). Asymmetry in barchans refers to one side of the crescent figure of a dune not mirroring the other side. The asymmetry of barchans is easily visible in the barchan horns because one horn is usually longer and wider than the other. This can be seen on the barchan in Figure 2 where the right horn is longer than the left horn.

Large barchans tend to display a more straight-line profile on their windward side than their smaller counterparts (Hastenrath, 1967). Barchans are most commonly observed to be 10 to 300 meters in width or length and 1 and 30 meters in height (Hersen, 2004; Cooke et al., 1993; Pye and Tsoar, 1990; Bagnold, 1941). Some barchans have even been observed to obtain heights up to 50 meters (Bourke and Goudie, 2009). Alternatively, barchans have not been observed on Earth to be smaller than 1 meter in height, which was first noted by Bagnold (1941). Andreotti et al. (2002) questioned how a barchan this small could form given its instability. The lack of observations regarding barchans approximating 1 meter in height indicate there a size limit to their formation (Hersen, 2004). This minimal limit is dependent on the interdune areas, the wind threshold velocity relationship, and the sand flux (Partelli et al., 2007).

Long and Sharp (1964) classified barchans into four distinct shapes (e.g. slim = 0.15 – 0.35, normal = 0.43 – 0.58, pudgy = 0.64 – 0.76, and fat = 0.89 – 2.02) by their a/c ratio, where a is the stoss slope length and c is the width between the horn tips.

These shape ratios were later reclassified by Bourke and Goudie (2009) to incorporate a wider range of values (e.g. slim = 0.125 – 0.375, normal = 0.376 – 0.625, pudgy = 0.626 – 0.875, and fat = 0.876 – >1.0) so more dunes that lie outside these bounds would now fit. When observing barchan fields through satellite imagery, it can be clearly observed that within each classification there are some instances of extreme examples. Most dunes within a field tend to share similar appearances, leaving barchans with exaggerated features to be distinct.

The size and shape of barchan horns can vary substantially from one dune to another. The magnitude of the barchan's asymmetry is represented by the inequity of horn length. The extended horn limb of the barchans dominant limb and can usually be classified into one of the following three groups: beaded, linear, and kinked (Bourke, 2010). Linear limbs are usually straight, while kinked limbs usually display a curved or angled morphology, and beaded limbs represent a line of beads extended in the downwind direction (Ping et al. 2016). Over time, if a horn continues to grow larger, then the more likely it is to lose sediment. Asymmetrical horn growth is due to a variety of factors including: sediment accretion, topography, dune interactions, and most prominently bidirectional wind regimes. (Bourke, 2010). As previously stated, barchans tend to usually form under near unidirectional winds. Occasionally, a bidirectional wind flow may occur preventing sand from accumulating or leaking uniformly, thus causing an asymmetric morphology to evolve. Bidirectional winds have a critical angle between them that determines which horn accretes sand and extends in the downwind direction (Ping et al., 2016). Zhang et al. (2018) suggests in some instances that dune collisions or an asymmetric sediment supply may be the largest factors influencing asymmetry. Simulations on horn morphology found in Parteli et al. (2014) support the influence of all these factors in some way.

Barchans in the Field

Barchans are usually found in groups that comprise part or all of a dune field (Worman et al., 2013). A barchan may influence the size and shape of other barchans downwind from it. The stability and growth of a barchan is usually due to the rate of sediment accretion (Durán et al., 2011). The horn tips of a barchan may leak sediment in the downwind direction providing a necessary influx for the next dune. At equilibrium, a barchan maintains its characteristic size and shape because the influx and outflux are equal. If either the influx or outflux of the sediment becomes greater than the other, then this could create dune instability, and cause the barchan to change its shape or size (Hersen and Douady, 2005). Larger barchans might continue to increase in size while smaller ones might decrease (Durán et al., 2011; Hersen, 2004).

Barchans are some of the fastest moving dunes in the world with their speed usually being inversely proportional to their size (Kroy et al., 2002). As dunes increase with height, they require more sand to move, and thus their rate of movement decreases (Mousavi et al. 2010). As previously stated, the sand accumulates near the top of the slip face, and over time, it eventually accumulates and avalanches down to the bottom of the the slip face. As the dune continuously repeats this process, it moves across the desert floor. Larger barchans take much longer to cross a dune field than smaller dunes. Often, smaller barchans will move fast enough to catch up and collide with the larger slower moving dunes downwind. Smaller barchans may calve off from the horns of the larger dune. This process might provide the opportunity for similarly sized barchans to appear throughout a dune field. Although, this is only possible if the smaller dune extracts a large enough portion of the mass from the parent dune to exhibit a characteristic size observed by other dunes found in the field (Diniega et al., 2010). Still though, similarly sized barchans seem to be apparent throughout dune fields.

When in large groups, barchans may form corridor like structures (Elbelrhiti et al., 2008). Worman et al. (2013) showed in their model that similarly sized dunes could emerge with scenarios as simple as the incoming and outgoing sand flux and the calving of smaller dunes from the horns of the larger ones. Additionally, size regulations may also occur through changes in wind direction and the collisions between dunes throughout the field (Elbelrhiti et al., 2008). This can be observed in well documented dune fields like the barchan field found near Tarfaya, Morocco. The denser regions seem to be populated by small barchans while diluted regions seem to be populated by larger barchans (Genois et al., 2013). Nonetheless, it is still of some debate how fields of similarly sized barchans can even emerge (Worman et al., 2013). Nonetheless, the factors controlling dune sizes is beyond the scope of this study.

Martian Barchans

Mars has a wind driven surface, allowing for a surplus of loose sediment and an abundance of dune systems (Greeley et al., 1992). Aeolian features are a valuable source for collecting data about the history of a planetary surface when ground observations are lacking (Bourke and Goudie, 2009). Barchans are representative of a period in the past when the planet shared a similarity of features found on Earth (Parteli and Herrmann, 2007; Breed et al., 1979). With satellite imagery, we have been provided the opportunity to study these dunes and other areas of the planet that rovers have not yet visited. Transverse and barchanoid dunes represent the dominant form of dunes on the Martian surface, a fact supported by visible wind streaks on the downwind side of the dunes (Malin et al., 1998; Lee and Thomas, 1995).

Additionally, most barchans seem to be larger on Mars than on Earth (Bourke et al., 2006), and seem to be predominantly composed of mafic minerals like pyroxene, which explains their naturally dark color (Tirsch and Jaumann, 2008).

On the Martian surface, we need to consider that the process of saltation might be different than that of Earth's due to the viscosity of the air around each grain, the properties of the grains, atmospheric conditions, gravity of Mars, and the velocity of the wind (Almeida et al., 2008). With the atmosphere being so thin, Martian winds should be strong enough for grain transportation (Parteli and Herrmann, 2007). Though previously thought to relics of past environmental conditions, the dunes on the Martian surface seem to be relatively active. With the advancement of cameras and the ability to record data with high resolution images, we can see that barchan surfaces are changing. Though more difficult than on Earth, under the right conditions, saltation can be initiated and continued under low flux conditions (Sullivan and Kok, 2017). Even coarse grains have been found to frequently move across the surface, despite previously recorded wind speeds still not being sufficient to dislodge the grains. (Baker et al. 2018). It is possible these heavier grains are moving through the process of creep instead of saltation. The wind speed and sand flux from the interdune area has been shown to affect the minimal dune size on the Martian surface (Parteli et al. 2006). With today's high-resolution imagery and an improved understanding of the grain movement on the surface, future research can address Martian barchan formation and morphology in better detail

METHODS

Study Sites

The study sites included in this research are listed in Table 1. This list includes a variety of dune fields with different barchan morphologies found on Google Earth and Mars. Dune fields were observed and selected using extensive literature research and Google earth observations. Data were collected from 19 dune fields and included more than 1500 barchans. Each dune field met the criteria described below in section: Dune Field Selection Criteria and had strong distinction between their features and the surrounding area to accurately obtain measurements. On Earth, both coastal and inland dune fields were analyzed, not giving any preference to geographical or topographical location. Every dune field in this study is different in that some are composed of only barchans or barchanoid complexes, and some dune fields have both barchans and other dune types. To clarify, barchanoid complexes within this study refer to multiple barchans that have a direct physical influence on each other (e.g. colliding). The boundaries selected for the study are the areas of the dune fields that contain only barchans.

Dune Field Selection Criteria

Each dune field in this study underwent the following observations before the barchan selection process began:

a) Dune field must contain stand-alone barchans somewhere within the field perimeter.

b) The image must display a high enough visual resolution to distinguish dune characteristics adequately. This is field dependent because each dune field is composed of different sized barchans.
c) If multiple images are used to cover a dune field, then each image must have the same date stamp.
d) The image must cover as much of the barchan portion of the field as possible.
e) The image must portray a low angle off nadir for most dunes.
f) Image should not contain any cloud cover over the barchan field.

Barchan Selection Criteria

Each barchan measured in this study had to meet the following criteria to be included (Figure 2):

a) A visually definable line between the dune base and the desert floor must be present.
b) Must possess a typical barchan crescentic shape (e.g. two identifiable horns, a clear stoss slope, and a defined slip face.). Refer to Figure 2 for reference.
c) Must not be part of a barchanoid complex.
d) Must not have any significant geomorphic irregularities that would alter any resulting measurements (see Figure 3).

If there were 100 barchans or fewer in a field, then the entire dune population was measured. If a field was composed of more than 100 dunes, then the dune population was subjected to a random selection process. The use of a random tessellation sampling approach allowed for the selection process to include barchans from the entirety of the field.

To eliminate a biased selection process, and to ensure complete randomness during selecting in this study, the use of a random-number generator and grid was implemented.

Sampling started by overlaying a grid image above a barchan field, starting from the most upwind measurable barchan (see Figure 4). The grid patterns were composed of at least 100 cells and were expanded to fit the entire measurable barchan field with the outermost barchans used as the grid boundary. Each cell should contain at least one barchan that met the criteria for the measurement process. Every cell within the grid was issued an unused number from 1 through 100, where sampling began from grid cell one. We chose the number of measured barchans to be 100 because it is twice the recommended amount by Andreotti et al. (2002). As stated above, if there was more than one barchan that met the measurement criteria within a cell, then the random number generator was used. Each barchan within the grid cell would be numbered sequentially, and then the random number generator would be used for the dune selection process. Once the selected dune was measured, that cell was crossed off, and the sampling process started over again in the next cell in the order. This process was repeated for each grid cell until 100 dunes were sampled from the field.

Measurements

This study used the ruler tool on Google Earth Pro for barchan measurements. Each barchan was measured by its length and width, which were broken up into a variety of sub-measurements (Figure 5). These include:

a) The length of the dune body from the slip face base to the stoss slope base. This line should be from the center of the innermost part of the slip face base to the center point of the stoss slope base (Line V).

b) The length of the slip face from the center of the innermost part of the slip face base to the brink line (Line Z).

c) The width of the dune at the base of the slip face (Line W).

d) The width of the gap between horn tip A and horn tip B (Line X).

The following parameters were also collected for each barchan outside the use of the ruler tool using observation or through simple calculation (Figure 5):

a) Barchan stoss side length.

Equation 1.

$$Y(m) = V(m) - Z(m)$$

b) Barchan height at the pinnacle of the brink (with the use of 32 degrees for the angle of repose).

Equation 2.

$$U(m) = \text{Tan}(32^{o}) \times Z(m)$$

c) Barchan morphology ratio (a/c). This study uses the Bourke and Goudie (2009) morphology classification (see section: Barchan Size).

Equation 3.

$$a/c\ ratio = \frac{Y(m)}{X(m)}$$

d) Apparent dominant horn limb.

e) Apparent dominant horn shape.

The barchans in this study displaying an asymmetric figure with one horn larger than the other were classified as having a dominant horn. For this study, an asymmetric barchan refers to a dune with unequal horn lengths in the downwind direction. The dominant horn was determined by which horn extended the furthest from the dune body in the downwind direction. The barchans that had horn A and horn B nearly the same length were classified as having no dominant horn. In this study, each barchan horn was labeled arbitrarily as horn A or B to make future identification easier. Before measurements began on each barchan, the dune was zoomed to and oriented so that the windward side faced the top of the screen and the horns pointed toward the screen's bottom. When observing the barchan from this above-view position, the horn on the left side of the barchan (on the left of the screen) was labeled as horn A and the horn on the right side was labeled horn B (see Figure 5). If horn A appeared to be longer than horn B, then horn A was considered to be the dominant horn and vice versa.

The use of the terms: small, medium, and large were used to provide a general description of barchan size. Medium sized barchans in this study are referred to roughly as the most commonly sized dunes in each field. The sizes pertaining to each category will vary from one field to another. The "small" classification in this scenario would contain all dunes in the field that fell below the medium size, while the "large" classification would be composed of barchans above the medium size.

Dune Field Comparison

Each dune field in this study had a different average size barchan (Figure 6). To compare these barchan fields with each other, we used the coefficient of variation, or *Cv* (Eq. 4):

Equation 4.

$$Cv\ (\%) = \left(\frac{STDV\ (m)}{\bar{X}\ (m)} \right) x\ 100$$

Where STDV is the standard deviation of the data set you are testing and $\bar{X}$ is the mean of the same data set. This equation provides a dimensionless number (the *Cv*), where the larger the number, the greater the discrepancy and variation is from the mean. The coefficient of variation of the width, length, height, and morphology were calculated for each dune field in Table 1. Then each value was graphed to determine dune field relationships and their similarity.

RESULTS

Over 1500 barchans were sampled from 19 different dune fields between Earth and Mars (Table 1.). Descriptive statistics for each field are summarized in Tables 2, 3, 4, and 5. An ANOVA test found that the dune fields were statistically significantly different (assuming a 95% confidence interval). Most barchans exhibited non-normal distributions with tails skewed to the right. The collective total distribution for the barchan fields of Earth portrayed the skewed right non-normality as well. Alternatively, though still slightly skewed, the barchan field near Arequipa, Peru and Ain Salah, Algeria presented a normal distribution. Arequipa was had a much higher value than Ain Salah though, with Ain Salah just above the required significance threshold.

The Martian barchan exhibited normal distributions apart from the dunes collected at Mclaughlin Crater and the Northern Polar Erg. These dune fields exhibited tails skewed to the right. Arkhangelsky Crater was the most normally distributed amongst all the dune fields researched in the study. The collective total distribution for the Martian fields showed a non-normal distribution, with a tail skewed to the right.

On average, the width, length, and height are usually linearly related to each other (Andreotti et al., 2002). This is confirmed to be the case with the data obtained in this study as well, although there is a slight difference between the level of relationships formed on Mars compared to those formed on Earth. This can be visibly viewed in the plot in Figure 13. Additionally, a Welch's T-test shows that the Martian and Earth populations regarding width and length are statistically significant from one another (p-value < 0.001). The relationships on Earth seemed to on average have a slightly higher R^2 value than those of Mars.

Additionally, the dune widths seem to be slightly smaller in relation to dune length on Mars than they do on Earth (Figure 13). The mean width on Earth and Mars is 90.4m and 199.7m, while the mean length is 64.3m and 227.8m (Mars).

Barchan fields on Earth showed a width coefficient of variation ranging between 25% and 89% with a mean of 51% The smallest coefficient of variation in width belonged to the dune field near Khovd, Mongolia, with the largest variation coming from the field south of Luderitz, Namibia. The Martian fields showed a range of *Cv* between 20% and 40%, with a mean of 29%. The smallest *Cv* comes from the dune field located in Arkhangelsky Crater while the largest is from the Northern Polar Erg swath. The coefficient of variation of the *Cv*'s on both Earth and Mars were relatively similar at 33% and 28% respectively. A summary of dune field main parameter statistics can be viewed in Tables 2, 3, 4, and 5.

Referring to the adjusted Long and Sharp (1964) morphology ratios from Bourke and Goudie (2009), which is discussed briefly in section: Barchan Size of this paper, showed that the morphological shape of barchans varied substantially between both Earth and Mars. Earth dune fields are composed largely of barchans that are morphologically pudgy (34.8%), followed closely by the fat (31.9%), and normal classification (27.2%). Martian dune fields were predominantly composed of fat barchans (83.5%). Both Earth and Mars had few slim barchans at 5.97% and 0.28%. The summary of barchan morphologies can be viewed in Figure 9.

The average dune width on Mars was found to be more than twice that of Earth. Additionally, the most common dune width on Earth was from 30m to 60m, while on Mars the most common width ranged from 90m to 220m. In total, 11 barchans had a width less than 10m with the lowest being 7m. Secondly, 19 barchans were shown to be smaller in height than 1m at the pinnacle of the brink line with the smallest being 0.7m.

Alternatively, the smallest Martian barchan displayed a cutoff around the 4m mark. The histograms outlining these data can be viewed in Figures 10, 11, and 12.

The morphology of the barchan horns varied between each planet. Of the total measured barchans on Earth, the dunes with a clear dominant limb occupied nearly 77% with horn A and horn B at a similar abundance of 37% and 40% respectively. Alternatively, the barchans on Mars favored horn A as the dominant horn at 39% compared to horn B at 25%. Collectively, the number of barchans with dominant horns were nearly equal with horn A and horn B at 38% and 37%. The dominant horns favored mostly a linear morphology at 68% with kinked less frequent at 31%. Both Earth and Mars favored a linear horn shape the most at 62% and 89%, with kinked coming in second at 36% and 10%. The beaded morphology was the least frequent amongst all dominant horns. These data can be viewed in Figure 8.

DISCUSSION

A t-test was performed to help validate that the barchan samples investigated in this study were representative of the fields they were found in. A field was chosen where all barchans were sampled, and where the population of the barchans in the field were as close to 100 as possible. A sample was then drawn from this field in the same manner that was performed in this study (just with a lesser quantity) and then was tested. The results show a p-value > 0.05 indicating that there is no significant difference between the sample and the actual field population.

The results in this study indicate that most barchan fields are not necessarily similar regarding the variation (*Cv*) of dune characteristics within each field. They seem to be slightly different based on the fact that the barchan fields sampled within this study had a coefficient of variation around 32%. If this *Cv* was at 10% or less, then maybe we could say the dune fields different barchan size populations share a similarity amongst each other. Since this is not the case though, with the resulting value being quite larger than this, it indicates the opposite scenario and suggesting barchan *Cv* vary quite largely from one field to another. Alternatively, many barchan fields showed some similarity with their distributions because most were skewed to the right. The skewed right histogram distributions were similar in appearance, but still varied slightly from one another. Still though, the distributions showed a high frequency of dunes clustering around a similar size (varies in each field). This indicates that most barchan populations have dunes of apparent similar size throughout their fields. When visually observing a field, it is difficult to mentally note a large difference from one size to another unless they are extreme examples of size differences.

A large *Cv* shows that even though barchans tend to cluster around a similar size in each field, the variation of the dunes within that field is actually quite significant.

Morphologically, a positive skew might show that most dune fields share an easier time accessing the earlier evolution stages of barchan formation while the well mature stages are more rare and difficult to obtain within any given dune field. This is visible in Figures 10, 11, and 12, where the frequency of barchan characteristics is much larger on the left side of the graph than on the right. Barchans may reach this size (varies in each dune field) relatively easily in dune evolution, but from that point on, they may have a difficult time accumulating enough sand to grow larger. We see in field models and observations (e.g. Worman et al. 2013; Duran et al. 2011; Elbelrhiti et al. 2008) that barchans form corridors structures composed of similarly sized dunes. Graphically, a positive skew might show the high frequency of the similarly sized dunes that are influencing each other, while the tail on the right might indicate the larger dunes outside the corridor's influences downwind. Either way, it was not a goal of this study to determine the cause of the similarly sized dunes or the factors controlling them.

Arequipa, Peru was the only sampled dune field that was different by showing a relatively normal distribution. The peak frequency for width was found to be near the 50-meter mark, which matches what Elbelrhiti et al. (2008) noted for the same dune field. The descriptive statistics for each barchan field can be found in Tables 2, 3, 4, and 5. Hastenrath (1967) stated that the barchans near Arequipa, Peru portrayed an amazingly well-formed crescentic shape. The observations included in this research support this statement. They have a well-defined shape and seem visually symmetrical most of the time.

The Arequipa barchans still change within the field though, providing a variation from the mean width, length, height, and morphology around 28.5%. This is one of the smallest *Cv* calculated in this study, but it still shows a relatively large set of different sizes prevalent throughout the field.

Alternatively, the largest variation occurred with the dune field near Luderitz, Namibia. This barchan field provided a *Cv* of nearly 85% in its width, length, and height, although the morphology variation was smaller at roughly 42%. Lancaster (1982) pointed out large differences between the different dune sizes within the field ranging from small normal dunes to large mega-barchans in some areas. This helps give a better comprehension of how the variation might be that high. The variations in Namibia include a wide range of complex morphologies within the field, which are surprisingly more than anyone would assume (Bourke and Goudie, 2009).

The *Cv* for Martian barchan characteristics (e.g. width, length, height, and morphology) was found to be lower than most *Cv* found for the Earth barchans. The *Cv* for the Martian barchan were also lower than the mean *Cv* for the combined dune fields from both planets (Figure 7). The barchans of Mars had on average lower coefficient of variations than that of Earth ranging between 20% and 40% where most fell below the average for the combined dune field variations (roughly 43%). It is of no question that Martian dunes are influenced under different environmental factors than those found on Earth. These differences (e.g. gravity, atmospheric conditions, grain properties, topography etc.) may provide alternate scenarios in which dune sizes on Mars are created and maintain less variation within their fields. Three of the five dune fields showed a normal distribution. For the fields that didn't have a normal distribution, they were once again skewed to the right.

The data show that few barchans are less than 1 meter high. The values calculated in these data are from the pinnacle of the brink line, which does not necessarily coincide with the crest of the dune. This doesn't provide a strong argument that these small dunes are actually less than 1 meter in total height. Additionally, image resolution is unlikely the cause for the lack of small barchans observed in this study because in most cases, the resolution was high enough to detect dune slip face lengths of just over a meter, which would put the height of the dune (pinnacle of the brink) near or just under a meter. The angle of repose used to calculate the height of barchans on Earth was also used to calculate the height of barchans on Mars. This was justified because Greeley et al. (1999) found an angle of repose on Mars of roughly 33^{o}, while Bourke et al. (2006) estimated an angle of repose at 32.4^{o}, and Atwood-Stone and McEwen (2013) found the angle of repose at three different Martian sites to fall between the $30^{o} – 35^{o}$ that's accepted for Earth dunes. The lack of barchans with heights smaller than 1 meter confirms a characteristic minimal size limit across all barchan fields (Hersen, 2004).

The asymmetrical morphology of barchans and their horns can be explained by different field characteristics including wind regimes, sand flux, topography, and dune interactions. In observation, most barchans are not symmetrical, even though some may be close. Additionally, all barchans sampled were categorized into the four morphologies created by Long and Sharp (1964) and edited by Bourke and Goudie (2009). Surprisingly though, the data in this study conflicts with the morphologies found on Mars by Bourke and Goodie (2009). Their results show that the northern polar sand seas favored slim, normal, and pudgy the most and in that order, while the intra-crater regions heavily favored slim and normal morphologies. The results presented in this paper (Figure 9) heavily favor fat and pudgy dunes in both the northern polar sand sea and the intra-crater areas.

Discrepancies between the two results may occur due to a variety of factors, but it is important to note that these differences may be largely due to study areas and a possible limitation within this study at the northern sand sea. Only one image swath was focused on for the northern polar sand sea instead of the entire northern erg. It is possible that this may have biased these results away from those of Bourke and Goodie (2009). Either way, it's clear that more observations are needed on Mars to achieve a better understanding of the wide diversity of dune morphologies present on its surface.

There are some important limiting factors that may have occurred during this study that need to be discussed. First, precision uncertainties may occur during the analysis of barchan images. Though great effort was made during the selection processes to make sure each section of the image would be as clear as possible, it's rare that everything would be perfect across the entire image at the same time. For some dunes in certain parts of the fields, the lighting and image resolution was near perfect for measurements to take place, allowing for better defined lines edging the different barchan characteristics. At other times though, in the same dune field, lighting or resolution may not have provided the same level of contrast noted previously on the other barchans. Additionally, resolution may have been nearly perfect for most dune sizes, but occasionally, smaller dunes would be presented, and thus be less defined at the same resolution. The issue regarding image resolution and lighting is estimated to provide an error no more than 3 – 5%.

A second source of uncertainty pertains to the measurement process during data collection. Besides the problems presented with image resolution and lighting previously mentioned, the measurement process is subjective to each person. Great care and time was taken into obtaining measurements from each barchan.

Each barchan was measured with line placement as close as possible to the exact point required to achieve true representative lengths and widths (see Figure 5 for measurements). Barchans in aerial or satellite imagery often exhibit crisp edges that help define their features, but in reality, these exact edges may vary slightly due to their edges being gradational in nature (Zhang et al. 2018). This may produce some error with placement of the end points of the measuring line. To help reduce this error, and before any measurements were taken, each barchan was enlarged as much as possible while still maintaining image structure. The level at which each barchan was zoomed to was different though, because image resolution and dune size varied from one field to another. The error associated with this manual practice was estimated around 3 – 5%.

A third source of error that may arise, which is also subjective, would be the orientation of the measured lines. The placement of lines over a barchan image in this study reflected the requirements found in section: Measurements (A, B, C, and D), and the visuals presented in Figure 5. When observing each barchan though, measured lines may be slightly off from true values (e.g. width measurement not being exactly perpendicular to the length measurement). The orientation of the width in this case would possibly give a slightly altered measurement that what would be found than if you measured exactly at line W in Figure 5. The steps in this study should allow anyone to obtain nearly identical measurements, but due to changes in orientation and the personal judgment of where the true edge of the dune is, would bias the values produced causing them to be slightly different. It is estimated that there might be a 5% error produced in this study representing exact barchan characteristic measurements based on the problems that emerge between image resolution and measured line placement or orientation.

A fourth source of uncertainty lies within the calculations. Barchan height in this study is found for the pinnacle of the brink line and not necessarily the crest.

It is unlikely that for each dune the pinnacle of the brink line and the crest of each barchan were the same. If they were not the same, then a slight discrepancy between the value calculated for height and the actual value may arise. Along with this problem, the value used for the slip face angle of all the dunes measured was 32 degrees. Though this is the most commonly accepted value for barchans, there still is a possibility that the slip face may have an angle outside this between 31 and 34 degrees. These alternate angles would not change the resulting heights too much, but it is still worth noting for future references. It is estimated that the error associated with this is estimated to be between 3 – 5%.

Fifth, each dune field was usually composed of multiple images. The dunes that were sampled came from images of the same date stamp. These date stamps were chosen based on the criteria listed in section: Dune Field Selection Criteria. Most images gave complete coverage of the entire dune field. Unfortunately, there were some images that had to be selected for analysis that excluded a small portion of the field, thus excluding dunes that may lay within that portion from contributing to this study. The estimated error caused by not using the entire field population is around 3%.

Lastly, the angle off nadir at which each image of the dune field was taken may cause slight alterations in measurements compared to in field observations. Although, it is unlikely that each sampled field had the same angle off center. Each image most likely has some portion of the dune field located directly below the camera. Being directly beneath the camera would obviously be the best scenario, but the study areas within this research are extremely large, so small errors in morphological values may occur the further the dune moves away from nadir. These errors should be negligible though because most images appear to be of narrow angle and had to meet the info found in section:

Dune Field Selection Criteria before measurements were obtained. The error associated with this is estimated to be around 1 – 3% given that most images were roughly the entire field.

CONCLUSION

Barchans are crescentic shaped dunes forming under near unidirectional winds and on hard, flat, sediment deprived surfaces. They are some of the fastest moving dunes in the world, and they can create an array of diverse interactions inducing a variety of field morphologies. The results presented in this paper, offer a unique snapshot view of the characteristics found in these dynamic dune fields. The results of this study are as follows:

The smallest *Cv* found amongst the barchan populations exhibited a 20% variation about the mean. This variation isn't the largest that could be expected, nor is it the largest that was found (e.g. 80% or more in one field), but still, with a *Cv* that large between some fields, the confidence to say that barchan fields share a similar coefficient of variation of sizes is rather absent. A large *Cv* indicates that a uniform size does not dominate any one field. Instead, each barchan population is composed of dunes with characteristics that show a variety of sizes.

Additionally, our results also indicate the presence of a characteristic minimal barchan size limit on both Earth and Mars. We can observe this in the sudden cutoff found in the histograms provided in this paper near the 10m width and length mark, and near the 1m height mark. This cutoff shows that barchans are nearly nonexistent below these levels in most dune fields, and that the barchan figure doesn't become apparent or evolve until it reaches these sizes. This size limit has been noted before by others, but this study helps confirm this limit is prevalent in most dune fields and increases the significance of the research and observations noted by previous scholars.

In this study we also bring forth the importance of the relationship between width, length, and height. Our results show that this relationship extends to nearly all barchans no matter which planet they occupy. The results also highlight that these relationships are slightly different on Earth than they are on Mars. Each dunes length seems to be longer on Mars at the same width of those found on Earth.

Barchan and horn morphologies showed that most fields seem to be composed of dunes with larger ratio values lingering around the pudgy and fat classification. Additionally, horns vary quite significantly, but show preference toward the linear characteristic in most dune fields on Earth and Mars. The Barchan body and horn morphologies covered by this study provide a glimpse as to what characteristics a barchan may maintain in the field, but it is still lacking in sufficient research and observations to draw final conclusions for all barchans.

It could be of great benefit to pursue in the future a mass morphological classification, larger than the one in this study, to help shed light on the wide variety of different barchan morphologies. It would also be beneficial to further explore and classify in more detail the different horn morphologies, including those of extreme extension and slight extension in the downwind direction, and to determine a threshold between each horn shape. Additionally, it would be useful to do a comparison analysis between barchans fields where each barchan is set to a relative size based on the largest barchan within their field. Hopefully, by highlighting some of the results in this paper, this research will kick start progress toward that direction and allow a better understanding of the basic barchan shape.

REFERENCES

Almeida M. P., Parteli J. r., Andrade J. S. Jr., Herrmann J. H. 2008. Giant Saltations on Mars. Proceedings of the National Academy of Sciences of the United States of America. 105, 6222 – 6226.

Andreotti B., Claudin P., Douady S. 2002. Selection of dune shapes and velocities Part 1: Dynamics of sand, wind, and barchans. European Physical Journal B. 28, 321 – 339.

Atwood-Stone C. and McEwen A. S. 2013. Measuring Dynamic Angle Of Repose In Low Gravity Environments Using Martian Sand Dunes. 44th Lunar and Planetary Science Conference. #1727.

Baker M. M., Newman C. E., Lapotre M. G. A., Sullivan R., Bridges N. T., Lewis K. W. 2018. Coarse sediment transport in the modern Martian environment. *J. Geophys. Res. Planets.* 123, 1380-1394.

Bagnold R. A. 1941. The Physics of Blown Sand and Desert Dunes. London, UK. Methuen and Co. Baird W. H., Padgett C. W., Secrest J. A. (2015). Google Earth Science. Physical Education. (50): 224.

Bourke M. C. 2010. Barchan dune asymmetry: Observations from Mars and Earth. Icarus. 205, 183 – 197.

Bourke M. C., Lancaster N., Fenton L. K., Parteli E. J. R., Zimbleman J. R., Radebaugh J. 2010. Extraterrestrial dunes: An introduction to the special issue on planetary dune systems. Geomorphology. 121, 1 – 14.

Bourke M. C., Goudie A. S. 2009. Varieties of barchan form in the Namib Desert and on Mars. Aeolian Research. 1, 45 – 54.

Bourke M. C., Balme M., Beyer R. A., Williams K. K., Zimbelman J. 2006. A comparison of methods used to estimate the height of sand dunes on Mars. Geomorphology. 81, 440 – 452.

Breed C. S., Grolier M. J., McCauley J. F. 1979. Morphology and Distribution of Common 'Sand' Dunes on Mars: Comparison with the Earth. Journal of geophysical research B. 84, 8183 – 8204.

Cooke R., Warren A., Goudie A. 1993. Desert Geomorphology. UCL Press.

Diniega S, Glasner K, Byrne S. 2010. Long-time evolution models of aeolian sand dune fields: Influence of dune formation and collision. Geomorphology. 121, 55 – 68

Dong Z., Qian G., Luo W., Wang, H. 2007. A wind tunnel simulation of the effects of stoss slope on the lee airflow pattern over a two-dimensional transverse dune. Journal of Geophysical Research: Earth Surface. 112, F03019.

Durán O., Schwämmle V., Lind P. G., Herrmann H. J. 2011. Size distribution and structure of Barchan dune fields. Nonlinear Processes in Geophysics. 18, 455 – 467.

Elbelrhiti H., Andreotti B., Claudin P. 2008. Barchan dune corridors: Field characterization and investigation of control parameters. Journal of Geophysical Research. 113, F02S15.

Génois M., Courrech du Pont S., Hersen P., Grégoire G. 2013. An agent-based model of dune interaction produces the emergence of patterns in deserts. Geophysical Research Letters. 40, 3909 – 3914.

Google Earth, obtained from, https://www.google.com/earth/, accessed Fall 2016 to Summer 2019.

Greeley R., Kraft M., Sullivan R., Wilson G., Bridges N., Herkenhoff K., Kuzmin R. O., Malin M., Ward W. 1999. Aeolian features and processes at the Mars Pathfinder landing site. Journal of Geophysical Research. 104, 8573 – 8584.

Greeley R., Lancaster N., Lee S., Thomas P. 1992. Martian Aeolian Processes, Sediments, and Features., Found in Kieffer H., Jakosky B. M., Snyder C. W., Matthews M. S. 1992, Mars. University of Arizona Press. 730 – 766.

Hastenrath S. L. 1967. The Barchans of the Arequipa Region, Southern Peru. Zeitschrift für Geomorphologie. 11, 300 – 311.

Hersen P., Dauady S. 2005. Collision of barchan dunes as a mechanism of size regulation. Geophysical Research Letters. 32, L21403.

Hesp P. A., Hastings k. 1998. Width, height and slope relationships and aerodynamic maintenance of barchans. Geomorphology. 22, 193–204.

Hersen P. 2004. On the crescentic shape of barchan dunes. The European Physical Journal B. 37, 507 – 514.

Kroy K., Fischer S., Benedikt O. 2005. The shape of barchan dunes. Journal of Physics: Condensed Matter. 17, S1229 – S1235.

Lancaster, N. 1995. Geomorphology of Desert Dunes. Boca Raton, Fla. Routledge.

Lancaster N. 1982. Dunes on the skeleton coast, Namibia (South West Africa): Geomorphology and grain size relationships. Earth Surface Processes and Landforms. 7, 575 – 587.

Lee P. L., Thomas P. C. 1995. Longitudinal Dunes on Mars: Relation to current wind regimes. Journal of Geophysical Research: Planets. 100.

Long J. T., Sharp R. P. 1964. Barchan Dune Movement In Imperial Valley, California. Geological Society of America Bulletin. 75, 149 – 156.

Malin M. C., Carr M. H., Danielson G. E., Davies M. E., Hartmann W. K., Ingersoll A. P., James P. B., Masursky H., McEwen A. S., Soderblom L. A., Thomas P., Veverka J., Caplinger M. A., Ravine M. A., Soulanille T. A., Warren J. L. 1998. Early Views of the Martian Surface from the Mars Orbiter Camera of Mars Global Surveyor. Science, News Series. 279, 1681 – 1685.

Mousavi S. H, Dorgouie M, Vali A. A, Pourkhosravani M, Ameri A. R. A. 2010. Statistical Modeling of Morphological Parameters of Barchan Dunes (Case Study: Chah Jam Erg in South of Haj Ali GHoli Playa, in Central Part of Semnan Province, Iran). Journal of Geography and Geology. 2.

Parteli, E. J. R.; Durán, O.; Bourke, M.C.; Tsoar, H.; Pöschel, T.; Herrmann, H. 2014. Origins of barchan dune asymmetry: Insights from numerical simulations. Aeolian Res. 12. 121–133.

Parteli E. J. R., Durán O., Tsoar H., Schwämmle V., Herrmann H. J., Stanley E. H. 2009. Dune Formation Under Bimodal Winds. Proceeding of the National Academy of Sciences of the United States of America. 106. 22085 – 22089.

Parteli E. J. R., Herrmann H. J. 2007. Dune formation on the present Mars. Physical Review E. 76, 041307.

Parteli E. J. R., Durán O., Herrmann H. J. 2007. Minimal size of a barchan dune. Physical Review E. 75, 011301.

Pelletier J. D., Sherman D. J., Ellis J. T., Farrell E. J., Jackson N. L., Li B. Nordstrom K. F., Maia L. P., Omidyeganeh M. 2015. Dynamics of sediment storage and release on aeolian dune slip faces: A field study in Jericoacoara, Brazil. Journal of Geophysical Research, Earth Surface. 120, 1911 – 1934.

Ping Lv., Dong Z., Narteau C., Rozier O. 2016. Morphodynamic mechanisms for the formation of asymmetric barchans: Improvement of the Bagnold and Tsoar models. Environmental Earth Sciences. 75, 259.

Pye K., Tsoar H. 1990. AEOLIAN SAND AND SAND DUNES. Unwin Hyman Limited, London. 396.

Sullivan R, Kok J. F. 2017. Aeolian saltation on Mars at low wind speeds. *J. Geophys. Res. Planets.* 122, 2111–2143.

Sutton S. L. F., McKenna Neuman C., Nickling W. 2013a. Lee slope sediment processes leading to avalanche initiation on an aeolian dune. Journal of Geophysical Research: Earth Surface. 118, 1754–1766.

Sutton S. L. F., McKenna Neuman C., Nickling W. 2013b, Avalanche grain flow on a simulated aeolian dune. Journal of Geophysical Research: Earth Surface. 118, 1767–1776.

Tsoar H., Parteli E. J. R. 2016. Bidirectional winds, barchan dune asymmetry and formation of seif dunes from barchans: a discussion. Environmental Earth Sciences. 75, 1237.

Tirsch D., Jaumann R. 2008. Mars: Dark intra – crater dunes on a regional scale. Planetary Dunes Workshop. 71 - 72.

Worman S., Murray A. B., Littlewood R., Andreotti B., Claudin P. 2013. Modeling emergent Large-scale structures of barchan dune fields. American Geophysical Union.

Zhang Z., Dong Z., Guangyin H., Parteli E. 2018. Migration and Morphology of Asymmetric Barchans in the Central Hexi Corridor of Northwest China. Geosciences. 8, 204.

APPENDIX

FIGURES

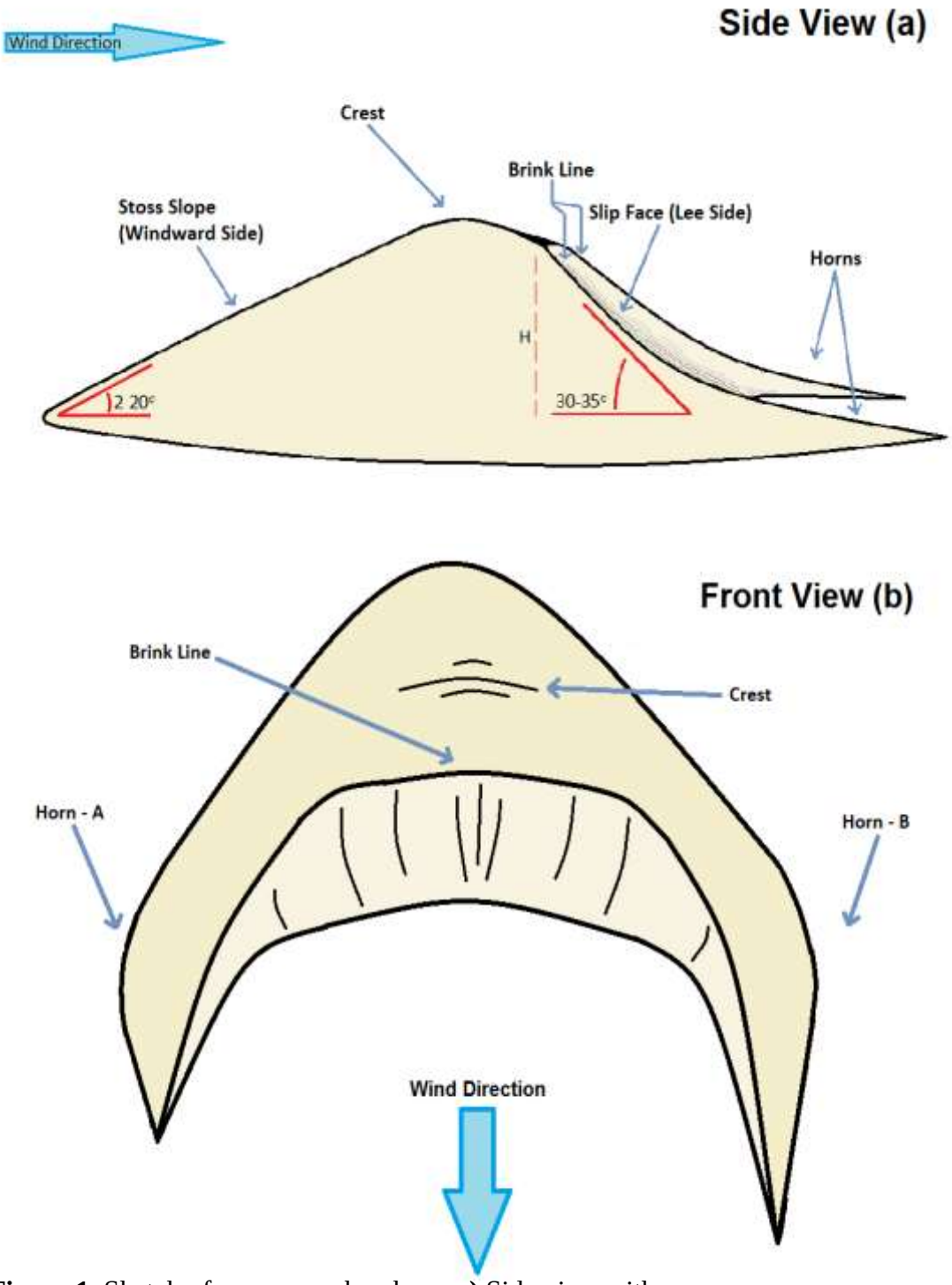

Figure 1. Sketch of a common barchan. **a.)** Side view with common barchan features and angles including stoss slope, crest, brink line, horns, and height (H). **b.)** Front view of a barchan and its common features.

Figure 2. An example of a barchan that fits the requirements of section: Barchan Selection Criteria. Image taken from the Namib Desert south of Luderitz, Namibia from Google Earth. Image info: Google Earth Pro. Imagery Date: 11/27/2012. Latitude: -26.830708, Longitude: 15.337108. 2019 Maxar Technologies. Accessed 08/21/2019.

Figure 3. An example of a barchan with geomorphic irregularities that separate it from classic dune characteristics. In this instance, the barchan imaged above would not have been measured for this study. Image taken from the Namib Desert from Google Earth. Image info: Google Earth Pro. Imagery Date: 02/02/2016. Latitude: -26.903679, Longitude: 15.347038. 2019 CNES/Airbus. Accessed 08/16/2019.

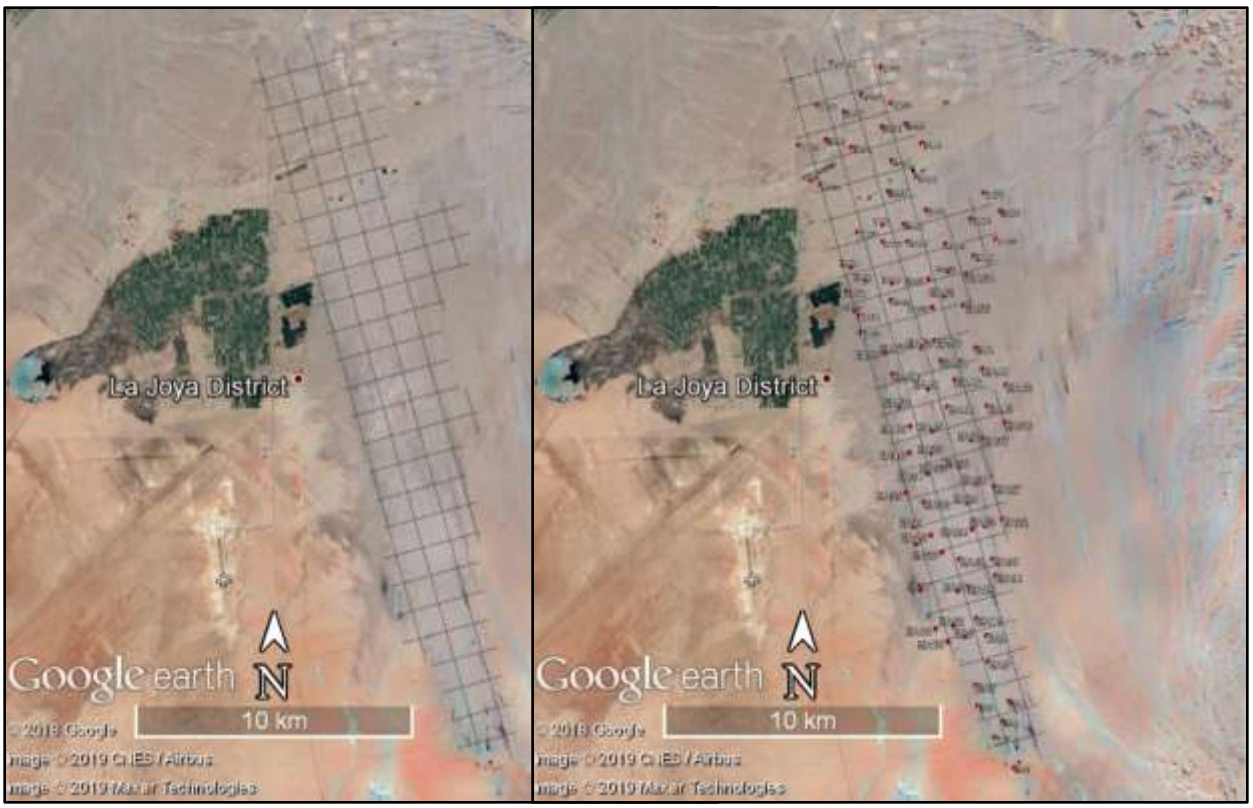

Figure 4. Shown above is the selection process with the use of a grid pattern on a dune field with more than 100 barchans (see section: Dune Field Selection Criteria). The outer dunes of the barchan field are first identified, and then a grid is generated and overlaid onto the field with the outer dunes as the grid's outer boundaries. Image taken next to the La Joya District near Arequipa, Peru. Image info: Google Earth Pro. Imagery Date: 07/08/2019. Latitude: -16.784651, Longitude: -71.816973. 2019 CNES/Airbus, 2019 Maxar Technologies. Accessed 08/013/2019.

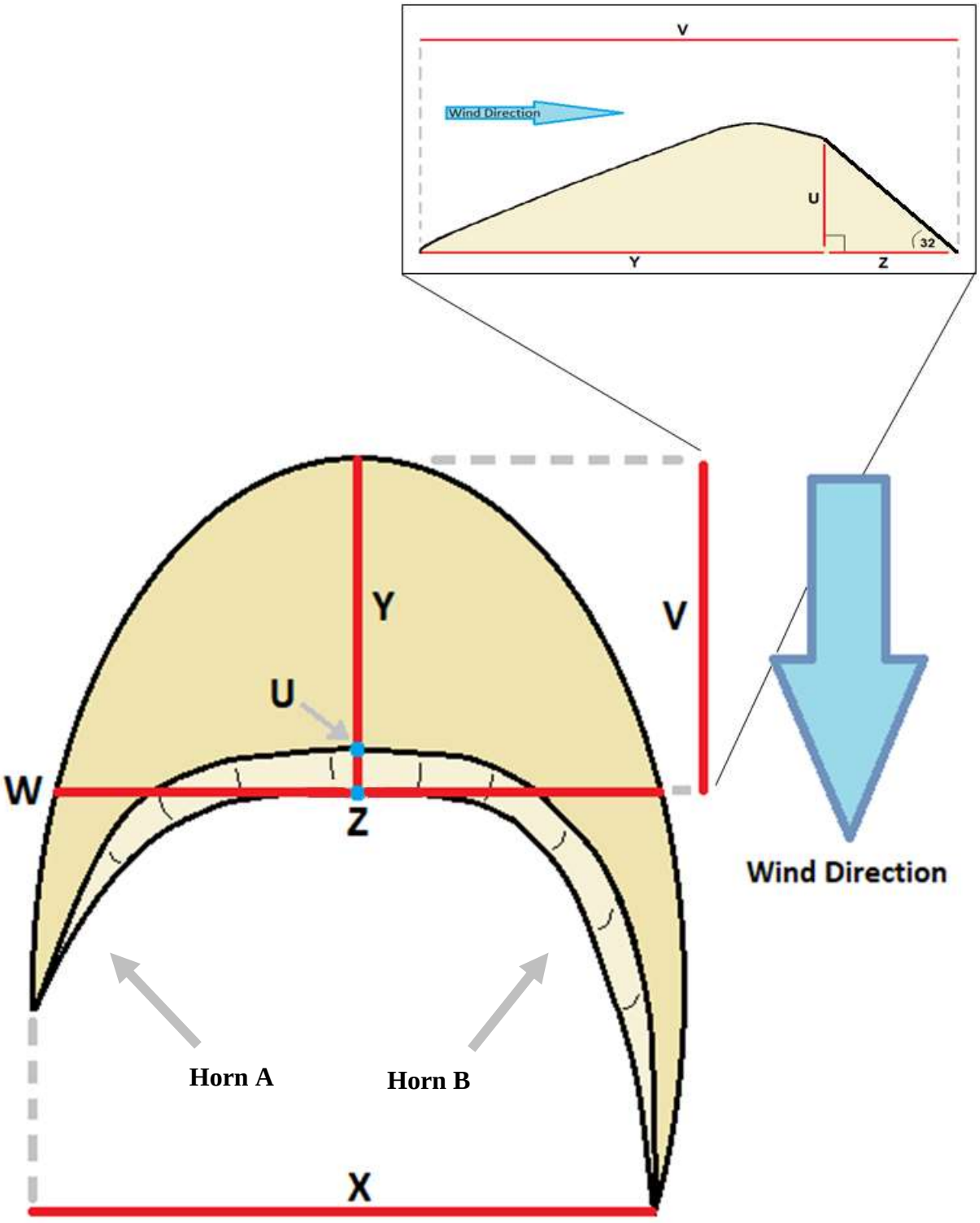

Figure 5. Measurements that were either obtained or calculated from the body of a barchan to complete this study, where W is the width of a barchan, Z is the length of the slip face, Y is the length of the stoss slope, X is the width between the two horns, U is the height at the pinnacle of the brink line, and V is the body length.

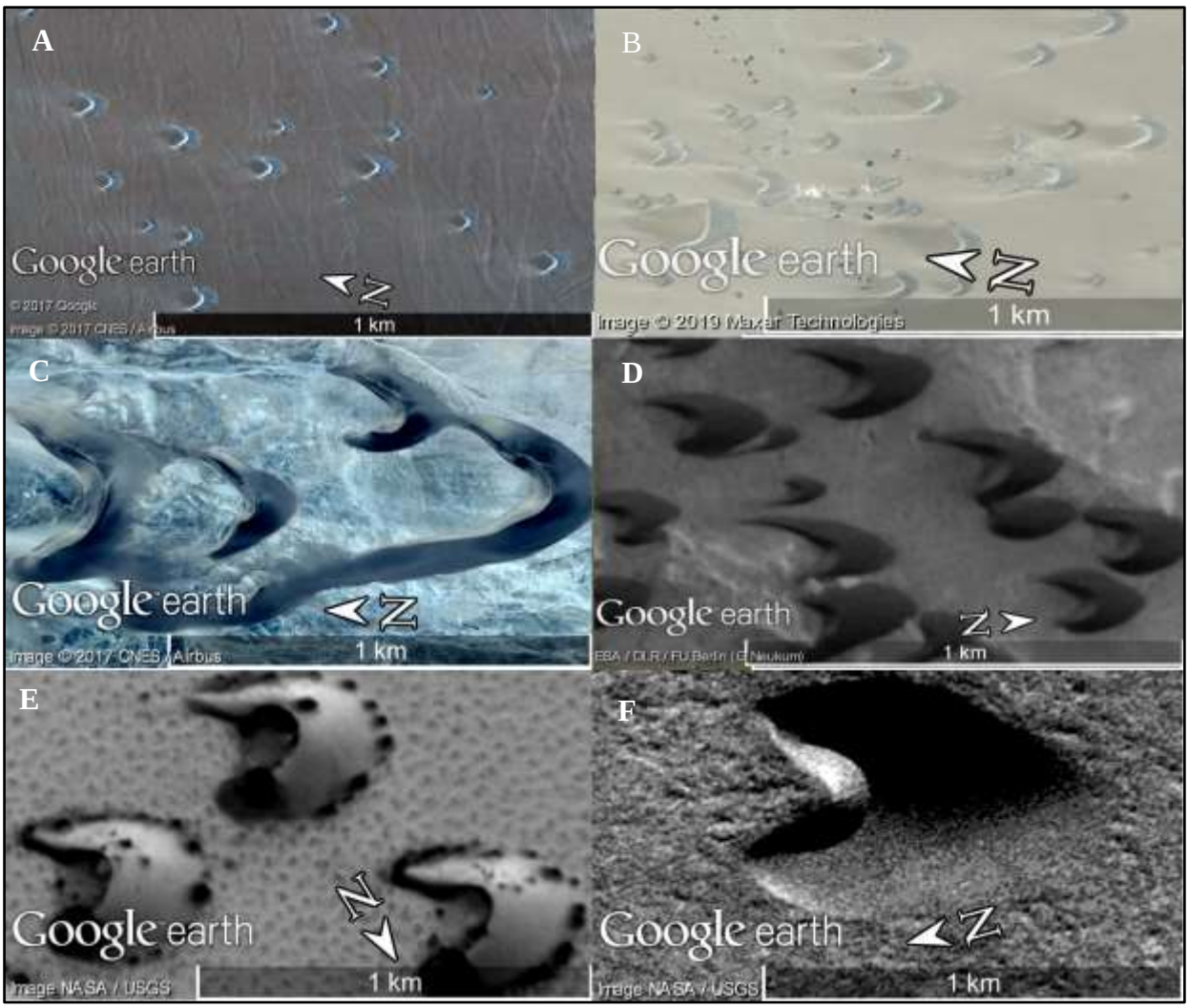

Figure 6. An example of the different scale of barchans found in different dune fields. A.) Image of barchans near Arequipa, Peru. B.) Image of barchans near Puerto Malabrigo, Peru. C.) Image of barchans near Luderitz, Namibia. D.) Image of barchans in McLaughlin Crater, Mars. E.) Image of barchans in the Northern Polar Erg, Mars. F.) Image of barchans in Arkhangelsky Crater, Mars. Images infor taken from Google Earth: A.) Google Earth Pro. Imagery Date: 08/16/2009. Latitude: -16.629887, Longitude: -71.940997. 2019 Maxar Technologies. B.) Google Earth Pro. Imagery Date: 02/01/2013. Latitude: -7.565108, Longitude: -79.426588. 2019 Maxar Technologies. C.) Google Earth Pro. Imagery Date: 02/02/2016. Latitude: -26.894602, Longitude: 15.324184. 2019 CNES/Airbus. D.) Google Earth Pro (Mars). Imagery Date: 2011. Latitude: -21.693810, Longitude: -22.582047. Mars Reconnaissance Orbiter CTX Imagery. NASA. ESA/DLR/FU Berlin (G. Neukum). E.) Google Earth Pro (Mars). Imagery Date: 2011. Latitude: -74.444374, Longitude: -53.248000. Mars Reconnaissance Orbiter CTX Imagery. NASA/USGS. F.) Image info: Google Earth Pro (Mars). Imagery Date: 2011. Latitude: -40.822571, Longitude: -24.939112. Mars Reconnaissance Orbiter CTX Imagery. NASA/USGS.

.

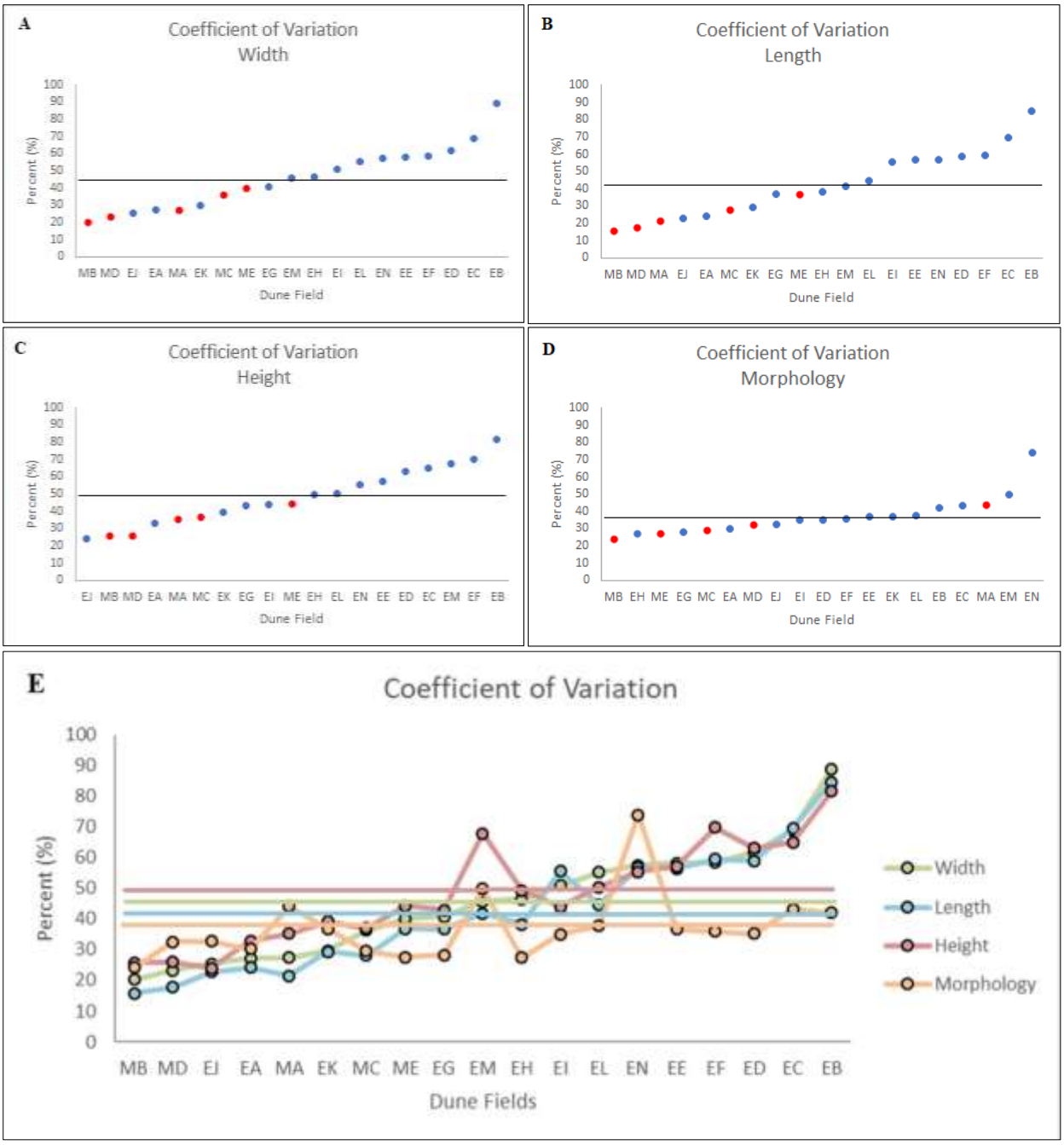

Figure 7. These graphs show the coefficient of variation (*Cv*) for the width, length, height, and morphology in each barchan field. The x-axis is ordered from left (lowest Cv) to right (highest Cv) with the listed dune fields shown in Table 1. In graphs A, B, C, and D, blue represents Earth and red represents Mars with the black line indicating the average. In graph E, the dune characteristics are shown against each other to visually compare their similarities. The colored horizontal lines represent the average *Cv* for that dune characteristic.

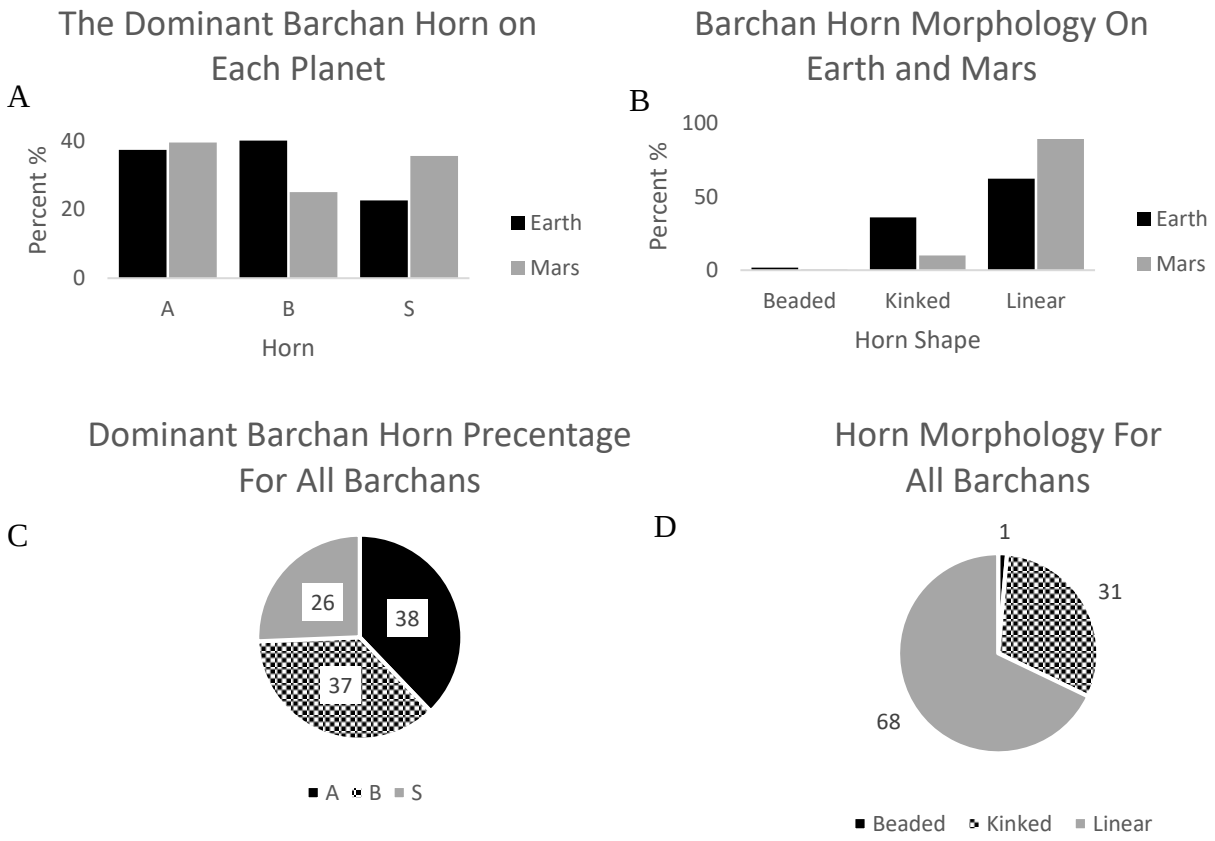

Figure 8. Statistical representations showing the differences in barchan and horn moprhologies. When observing a barchan from the above-view looking down, horn A is on the left side of the barchan while horn B is on the right. The S label refers to barchans whose horns were of similar length and didn't show a clear dominant horn. Graph A shows which horn was most dominant on barchans from Earth and Mars. Graph B shows which morphologies the dominant horn represented from Earth and Mars. Graph C shows which horn was dominant among all the dunes measured. Graph D shows which morphologies was the most common among all the dunes measured.

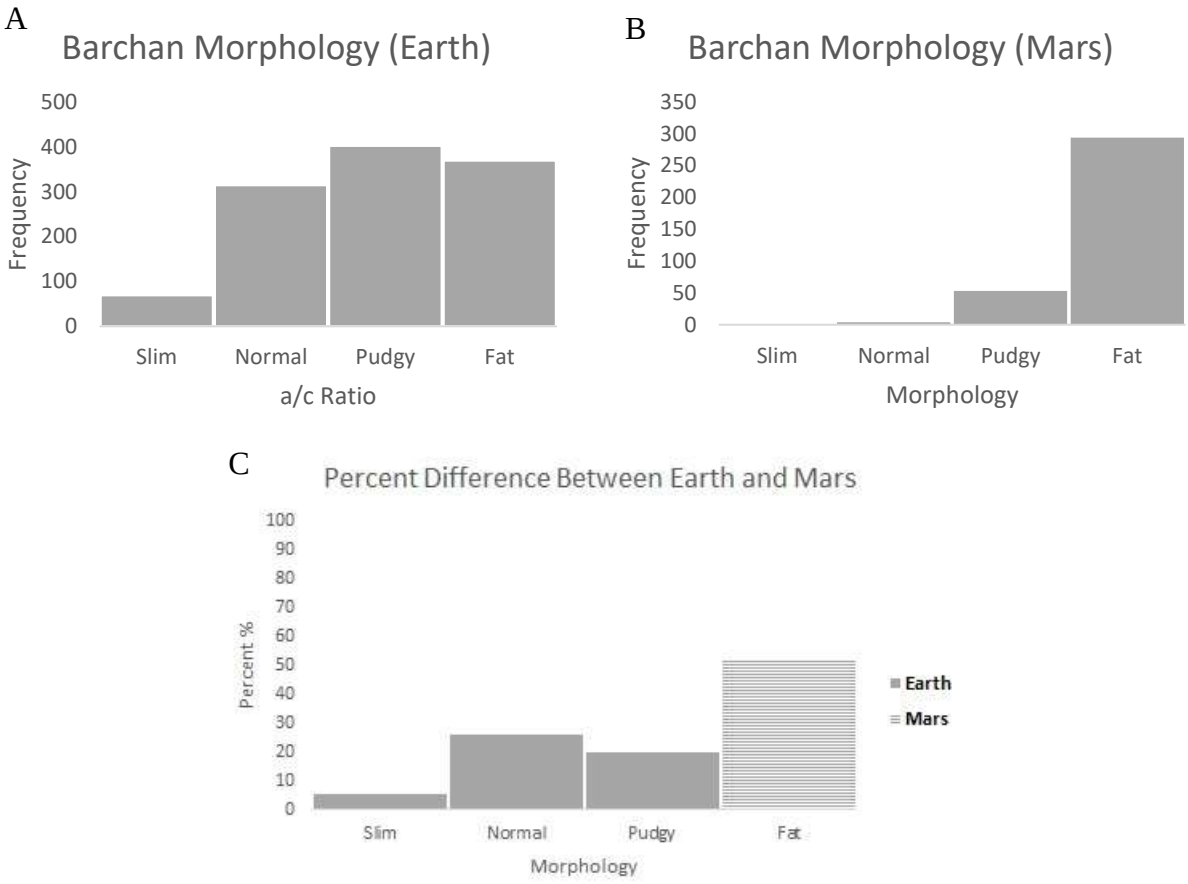

Figure 9. Barchan morphologies and their differences on each planet. Graph A shows the frequency of each barchan morphology on Earth while graph B shows the frequency on Mars. Graph C shows the percent difference between Earth and Mars for each morphology with the color indicating which planet contained the larger quantity.

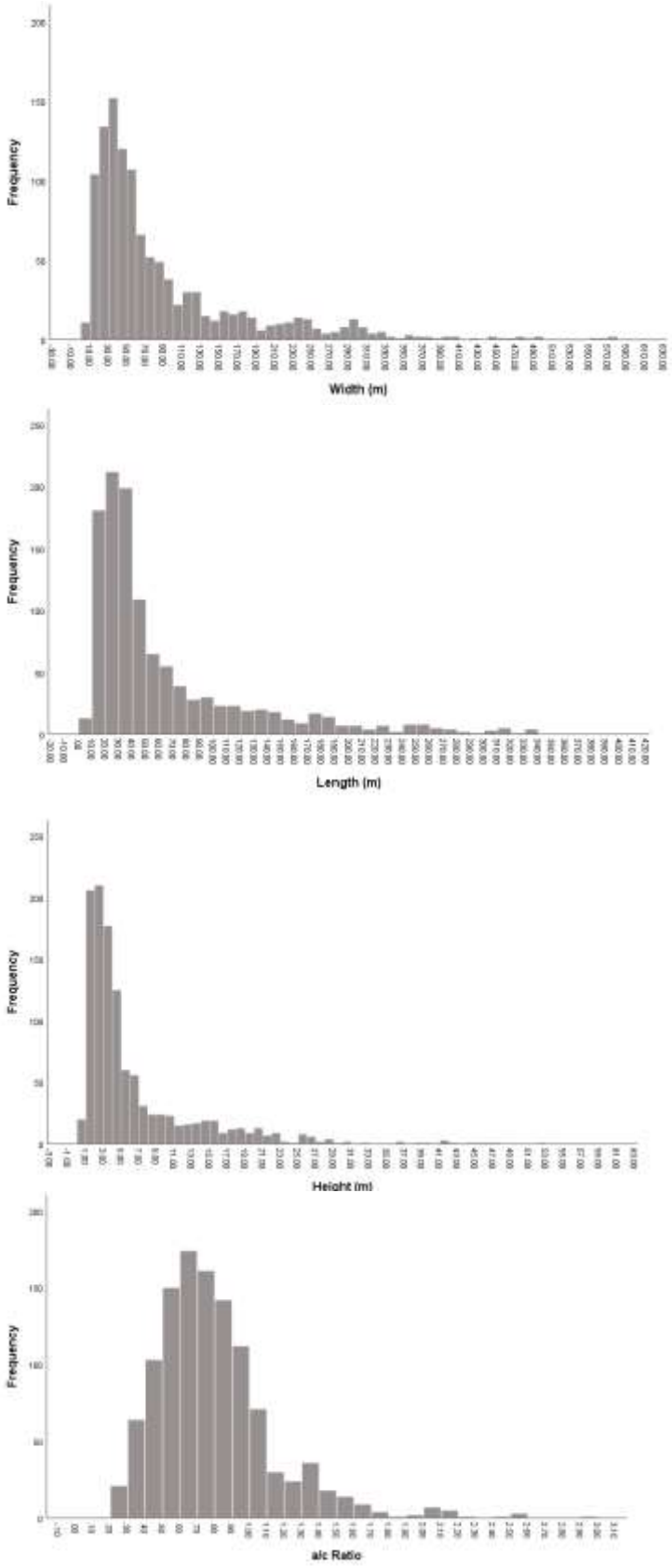

Figure 10. Histograms of all the Earth dunes with characteristics focused on width, length, height, and morphology.

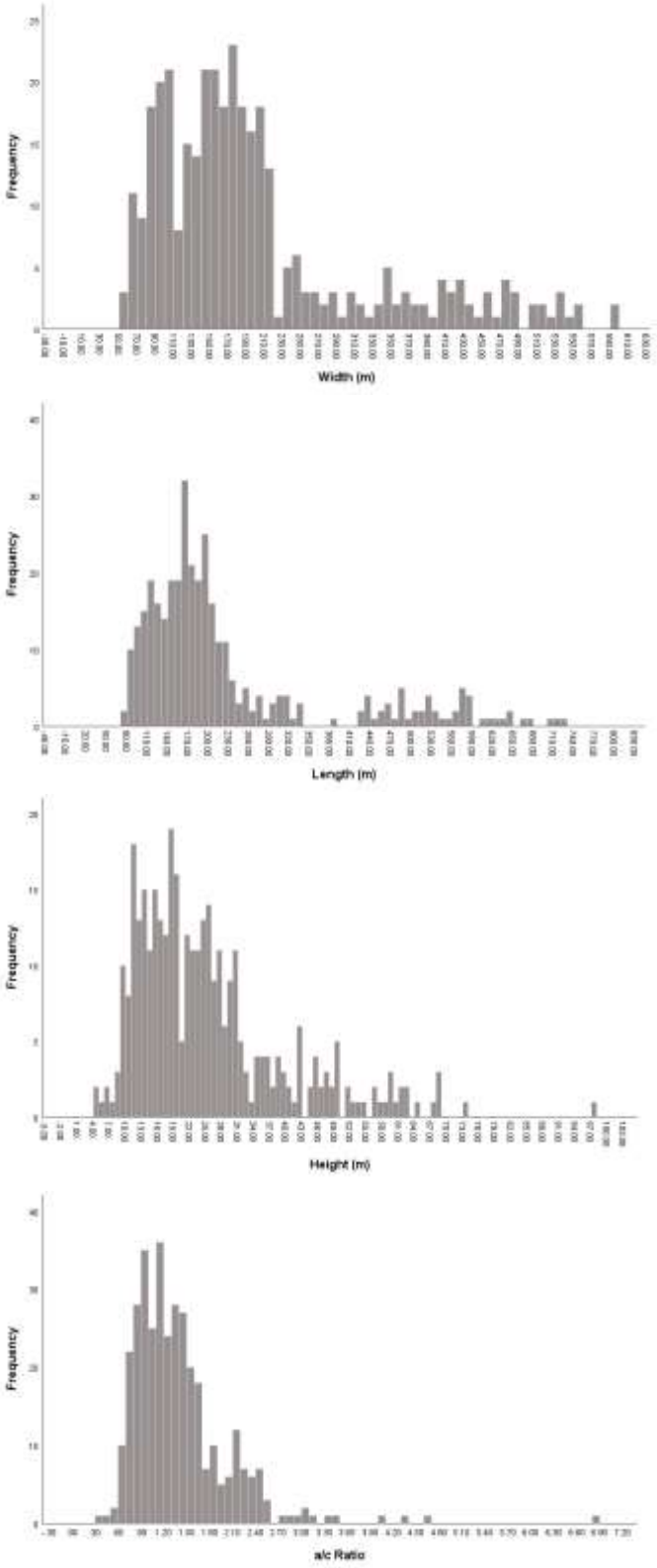

Figure 11. Histograms of all the Martian dunes with characteristics focused on width, length, height, and morphology.

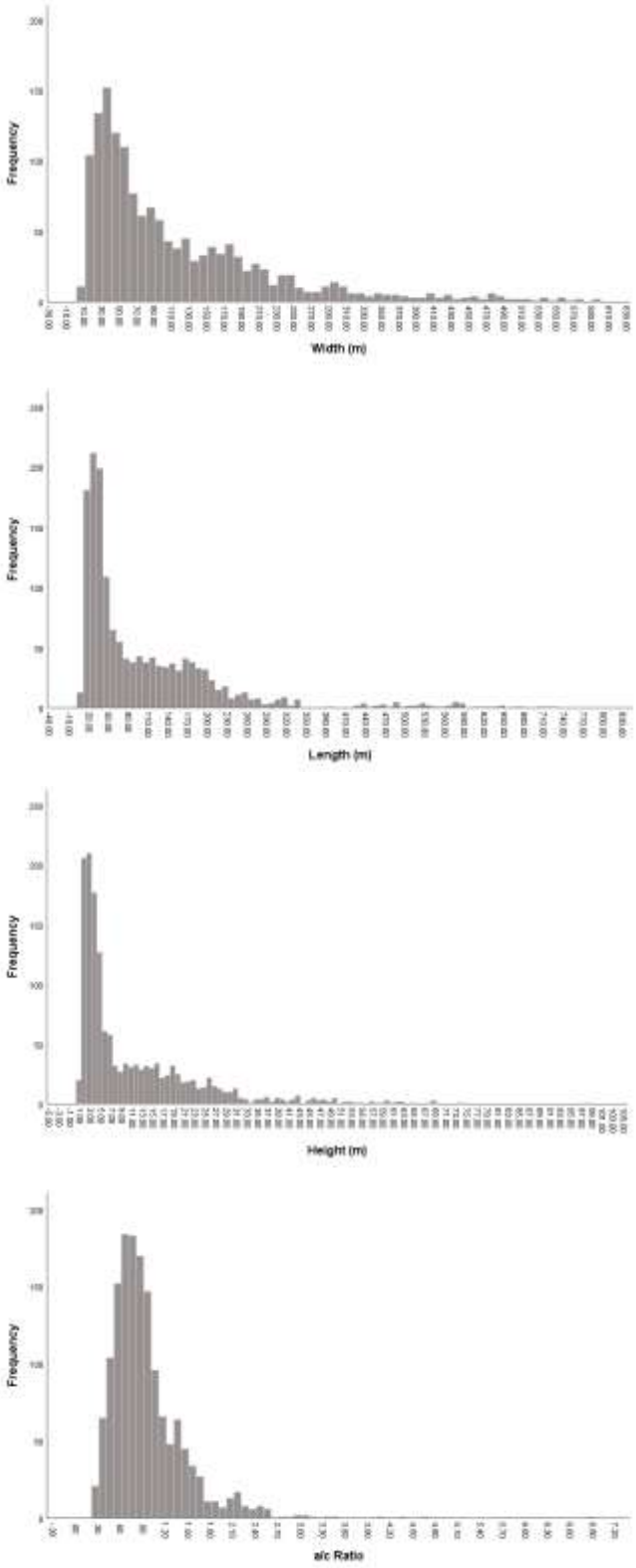

Figure 12. Histograms of all the dunes with characteristics focused on width, length, height, and morphology.

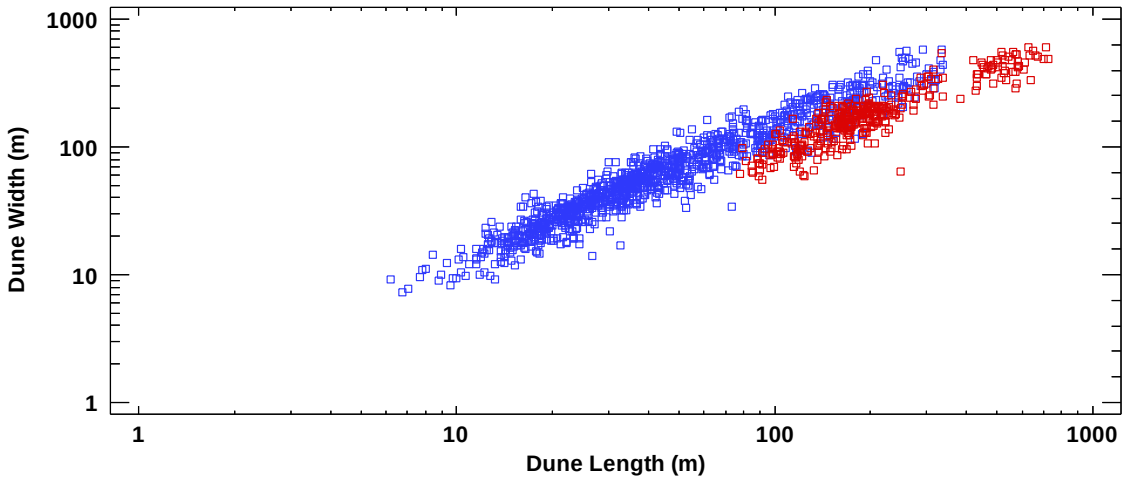

Figure 13. Plot showing the linear relationship between length and width with a correlation coefficient (R^2) on Mars at 92.4% (p-value < 0.001) and on Earth at 93.7% (p < 0.001). Barchans populations on Earth are colored in blue while those of Mars are colored in red. This plot highlights that the barchans on each planet share a slightly different relationship in their characteristics causing a visible difference in the above figure.

TABLES

Table 1. List of barchan dune fields in this study.

Planet	Country	Geographical Area	Field I.D.	Latitude	Longitude
Earth	Peru	Arequipa	EA	-16.852876	-71.797508
Earth	Namibia	Luderitz	EB	-27.604953	15.549455
Earth	Chad	Faya - Largeau	EC	17.990165	19.395299
Earth	Qatar	Mesaieed	ED	25.085199	51.367558
Earth	Yemen	Al Huwaymi	EE	13.986216	47.815000
Earth	Peru	Nazca	EF	-15.141580	-75.255013
Earth	Peru	Quita Sombrero	EG	-9.9083290	-78.222026
Earth	Peru	Puerto Malabrigo	EH	-7.6539570	-79.414057
Earth	Egypt	Kharga	EI	25.749371	30.351083
Earth	Mongolia	Khovd	EJ	48.168928	93.717993
Earth	Australia	Kalbarri	EK	-26.826797	113.719713
Earth	Peru	Piura	EL	-6.0770870	-80.920746
Earth	Algeria	Ain Salah	EM	27.215800	2.5427920
Earth	Peru	Casma District	EN	-9.4203570	-78.387188
Mars	N/A	Western Hellas Planitia	MA	-41.453080	44.613418
Mars	N/A	Arkhangelsky Crater	MB	-40.919949	-25.047155
Mars	N/A	McLaughlin Crater	MC	21.737424	-22.671996
Mars	N/A	Crater NW of Trouvelot	MD	17.787816	-17.016177
Mars	N/A	Northern Polar Erg Swath	ME	74.828707	-54.113620

Table 2. Descriptive Statistics on barchan widths (m) within each dune field. The coefficient of variation (*Cv*) is listed as a percent.

Field I.D.	EA	EB	EC	ED	EE	EF	EG	EH	EI	EJ	EK	EL	EM	EN	MA	MB	MC	MD	ME
Mean	45	115	134	220	91	40	30	39	182	76	83	25	127	33	118	423	121	198	218
Median	47	65	124	187	76	34	27	34	160	73	80	22	121	29	117	424	108	196	189
Std. Deviation	12	102	92	136	53	23	12	18	93	19	24	14	58	19	32	86	44	46	87
Minimum	14	16	13	35	21	10	14	13	34	48	53	7	36	8	59	236	55	107	117
Maximum	85	472	399	578	238	112	63	81	410	137	153	82	289	90	194	599	264	347	596
Range	72	456	386	543	217	102	50	68	375	89	100	75	253	83	134	363	209	240	479
Cv	27	89	69	62	58	59	41	46	51	25	30	55	46	57	27	20	36	23	40

Table 3. Descriptive Statistics on barchan lengths (m) within each dune field. The coefficient of variation (*Cv*) is listed as a percent.

Field I.D.	EA	EB	EC	ED	EE	EF	EG	EH	EI	EJ	EK	EL	EM	EN	MA	MB	MC	MD	ME
Mean	31	72	117	128	59	30	25	26	143	46	60	22	104	28	162	539	129	210	220
Median	32	42	111	113	49	25	22	23	119	45	56	22	98	23	161	530	120	199	193
Std. Deviation	7	61	82	75	33	18	9	10	80	10	18	10	43	16	35	85	36	37	81
Minimum	12	10	10	20	15	8	14	12	26	29	35	7	36	6	98	308	78	155	114
Maximum	48	338	331	337	174	91	46	58	318	90	109	58	230	76	250	723	251	316	630
Range	36	327	321	316	158	84	32	46	292	62	74	51	193	70	152	415	173	161	516
Cv	24	85	70	59	57	59	37	38	55	23	29	45	42	57	21	16	28	18	37

Table 4. Descriptive Statistics on barchan heights (m) within each dune field. The coefficient of variation (*Cv*) is listed as a percent.

Field I.D.	EA	EB	EC	ED	EE	EF	EG	EH	EI	EJ	EK	EL	EM	EN	MA	MB	MC	MD	ME
Mean	3.1	9.6	9.5	18.6	4.9	2.5	2.5	3.1	12.6	3.9	4.4	2.2	5.1	2.5	14.5	44.7	17.2	21.5	32.0
Median	3.1	5.8	8.5	15.7	4.2	2.0	2.2	2.8	11.8	4.0	4.2	1.9	4.5	2.2	14.7	44.7	15.1	21.2	27.6
Std. Deviation	1.0	7.8	6.2	11.7	2.8	1.7	1.1	1.6	5.5	0.9	1.7	1.1	3.4	1.4	5.1	11.5	6.4	5.6	14.2
Minimum	0.9	1.1	0.8	3.2	1.3	0.7	1.1	1.0	3.3	1.6	1.6	0.9	1.4	0.7	4.1	21.4	7.0	10.2	12.7
Maximum	6.8	29.3	25.9	52.1	15.1	9.5	5.1	7.6	28.6	7.8	8.2	6.5	15.9	7.7	27.8	73.3	38.4	35.0	97.9
Range	5.9	28.2	25.1	48.9	13.7	8.8	4.0	6.7	25.3	6.2	6.6	5.7	14.5	7.0	23.7	51.9	31.4	24.8	85.3
Cv	32.9	81.6	65.1	63.0	57.2	69.9	43.0	49.3	43.9	23.9	39.1	50.5	67.8	55.3	35.3	25.8	37.0	26.0	44.3

Table 5. Descriptive Statistics on barchan morphology within each dune field. The coefficient of variation (*Cv*) is listed as a percent.

Field I.D.	EA	EB	EC	ED	EE	EF	EG	EH	EI	EJ	EK	EL	EM	EN	MA	MB	MC	MD	ME
Mean	0.80	0.61	0.79	0.46	0.60	0.83	0.83	0.71	0.87	1.05	0.78	1.16	1.03	0.93	2.17	1.76	1.14	1.38	1.03
Median	0.74	0.56	0.74	0.43	0.57	0.77	0.81	0.67	0.82	0.97	0.62	1.03	0.89	0.84	2.03	1.69	1.14	1.35	0.99
Std. Deviation	0.24	0.26	0.34	0.16	0.22	0.30	0.23	0.20	0.31	0.34	0.29	0.44	0.51	0.33	0.96	0.43	0.34	0.45	0.28
Minimum	0.48	0.28	0.27	0.20	0.20	0.40	0.41	0.41	0.37	0.44	0.45	0.53	0.34	0.44	1.15	1.06	0.62	0.73	0.33
Maximum	2.01	2.06	2.91	1.04	1.08	2.11	1.54	1.42	2.10	2.51	1.29	2.48	2.54	2.51	6.84	3.08	2.41	2.89	2.18
Range	1.53	1.78	2.63	0.84	0.88	1.71	1.13	1.01	1.73	2.08	0.85	1.95	2.20	2.08	5.69	2.03	1.79	2.16	1.84
Cv	30.19	41.95	43.32	35.21	36.74	35.87	28.27	27.29	35.11	32.70	36.91	37.69	49.92	35.22	44.15	24.14	29.49	32.64	27.58